Pure appl. geophys. 160 (2003) 717–737
0033–4553/03/040717–21

Pure and Applied Geophysics

Seismic Tomography of the Lithosphere with Body Waves

CLIFFORD H. THURBER[1]

Abstract — A pair of papers in 1976 lead-authored by Kei Aki heralded the beginning of the field of seismic tomography of the lithosphere. The 1976 paper by Aki, Christoffersson, and Husebye introduced a simple and approximate yet elegant technique for using body-wave arrival times from teleseismic earthquakes to infer the three-dimensional (3-D) seismic velocity heterogeneities beneath a seismic array or network (teleseismic tomography). Similarly, a 1976 paper by Aki and Lee presented a method for inferring 3-D structure beneath a seismic network using body-wave arrival times from local earthquakes (local earthquake tomography). Following these landmark papers, many dozens of papers and numerous books have been published presenting exciting applications of and/or innovative improvements to the methods of teleseismic and local earthquake tomography, many by Aki's students.

This paper presents a brief review of these two types of tomography methods, discussing some of the underlying assumptions and limitations. Thereafter some of the significant methodological developments are traced over the past two and a half decades, and some of the applications of tomography that have reaped the benefits of these developments are highlighted. One focus is on the steady improvement in structural resolution and inference power brought about by the increased number and quality of seismic stations, and in particular the value of utilizing shear waves. The paper concludes by discussing exciting new scientific projects in which seismic tomography will play a major role — the San Andreas Fault Observatory at Depth (SAFOD) and USArray, the initial components of Earthscope.

Key words: Tomography, body waves, teleseismic, local earthquake.

Introduction

In 1974, Kei Aki visited NORSAR, and the availability of high-quality seismic data from a dense array combined with Aki's knowledge of inverse theory led to the "birth" of modern seismic tomography. Working together with A. Christoffersson and E. Husebye, the three developed what has become known as the ACH teleseismic tomography method. The method uses the arrival times of *P* waves at a seismic array or network to infer three-dimensional (3-D) velocity heterogeneities in the volume beneath the stations. The team published their analyses of data from 2 arrays and one regional network in 3 papers that appeared in 1976 and 1977 (AKI *et al.*, 1976, 1977; HUSEBYE *et al.*, 1976). As the story goes, the third paper in the series, which is the one most widely cited, was intended to be published first, but a sign error in the

[1]Department of Geology and Geophysics, University of Wisconsin-Madison, 1215 W. Dayton St., Madison WI 53706, U.S.A. E-mail: thurber@geology.wisc.edu

data delayed its publication (EVANS and ACHAUER, 1993). Then in 1975, Aki spent time at the U.S. Geological Survey in Menlo Park, California. Working together with Willie Lee, the pair extended the ACH tomography method to the case of local earthquakes. The local earthquake method utilizes *P*-wave arrival times from earthquakes beneath a seismic network to infer the 3-D velocity structure in the volume containing the earthquakes and stations. Their local earthquake tomography paper was published in 1976 (AKI and LEE, 1976). I will refer to their approach as the A&L method.

The author was fortunate to arrive at MIT in the fall of 1976. A number of graduate students, both of Aki's and of other faculty members, was either already or soon to be working on applications of seismic tomography (although we did not call it tomography at the time). Among this group were Bill Ellsworth, George Zandt, Steve Roecker, Steve Taylor and myself. Computers at MIT were slowly making the transition from punched cards to on-line disk storage and remote terminals, and color graphics were done with Exacto knives and colored acetate sheets. How times have changed!

The retirement of Kei Aki brings an opportunity to reflect on the brief history of seismic tomography using body waves, with a focus on work involving his students and their collaborators. The initial tomography methods made simplifying assumptions that have become generally unnecessary due to advances in methodology and computer power. Local- and regional-scale applications were initially limited to places where seismic arrays or networks were in place. However, the creation of the Incorporated Research Institutions for Seismology (IRIS) portable seismic instrument program, the Program for Array Seismic Studies of the Continental Lithosphere (PASSCAL) (SMITH, 1986; FOWLER and PAVLIS, 1994), opened up virtually unlimited opportunities for carrying out tomography studies in regions of scientific interest. Now there may be the beginning of a new era of opportunity for seismic tomography studies in the U.S. with the impending establishment of the Earthscope program (HENYEY *et al.*, 2000). With tomography components ranging from the fine-scale structure of the San Andreas fault in the SAFOD project to the broad-scale structure of the North American lithosphere in the USArray project, Earthscope promises to provide the field of seismic tomography with unprecedented data for imaging the internal structure of the earth.

Basic Tomography Methodology

Both teleseismic and local earthquake tomography make use of the arrival times of body waves (*P* and/or *S*) to infer the seismic velocity structure. In the case of teleseismic tomography, the earthquakes must be at relatively great distances from a localized cluster of seismic stations, so that the waves incident on the array can be treated as plane waves (Fig. 1a). With this assumption, it is only the structure

immediately beneath the stations that contributes to arrival time perturbations (relative to a radially-symmetric model), and the source locations and origin times need not be precisely known. I note that this assumption has been questioned by MASSON and TRAMPERT (1997), who showed that travel times to the base of an ACH model through a representative global 3-D velocity model could not adequately be treated as a plane wave in some cases. However, this potential problem can be avoided using the approach of WIDIYANTORO and VAN DER HILST (1997) or BIJWAARD *et al.* (1998), by modeling coarse-scale global structure and fine-scale regional structure simultaneously. In contrast, for local earthquake tomography, the events and stations are in the same area (Fig. 1b). In this case, structure along the entire path from event to station contributes to arrival time perturbations, and the source location and origin time need to be treated formally as unknowns along with the structure model.

For teleseismic tomography, the equations are written to separate the contributions to arrival time from inside versus outside the model:

$$t = \bar{\tau} + \sum_{s=1}^{NL} \bar{t}_s \sum_{k=1}^{M} F_{sk} \left(1 + \frac{\Delta u_k}{u_s} \right) + \varepsilon \tag{1}$$

where t is the arrival time at the station, $\bar{\tau}$ is the arrival time at the base of the model (calculated from a standard earth model), $\bar{t}_s$ is the travel time through layer s in the unperturbed medium, F_{sk} is 1 if the ray in layer s has most of its length in block k and is otherwise zero, u_s is the slowness in layer s, Δu_k is the slowness perturbation in block k, and ε represents model errors and measurement errors. AKI *et al.* (1977) expressed this in matrix notation for a set of observations as

$$\mathbf{t} = \bar{\tau} - \mathbf{G}\bar{\mathbf{m}} + m_0\mathbf{i} + \varepsilon \tag{2}$$

where $\mathbf{t}$ is the vector of arrival times,$\bar{\tau}$ is the vector of arrival times at the base of the model, $\mathbf{G}$ is the relatively sparse matrix containing the appropriate $\bar{t}_s$ values, $\bar{\mathbf{m}}$ is the vector of fractional slowness deviations from the layer average in the blocks, m_0 is the travel time through the unperturbed model, $\mathbf{i}$ is a vector consisting of ones, and the vector ε contains the error terms. By rewriting equation (2) in terms of arrival time residuals and subtracting the average of the travel time residual over all stations for each event from the left-hand side, Aki and Lee arrived at the relation

$$\mathbf{t}^* = \mathbf{G}^*\bar{\mathbf{m}} + \varepsilon^* \tag{3}$$

where * indicates the vector or matrix value minus the corresponding average. Thus the ACH method inverts relative arrival time residuals for relative perturbations in fractional slowness. This approach effectively removes error contributions from inaccuracies in the standard earth model and in the source location and origin time.

For local earthquake tomography, the derivation of the equations is simpler because no averaging is required to remove the source and outside-the-model path

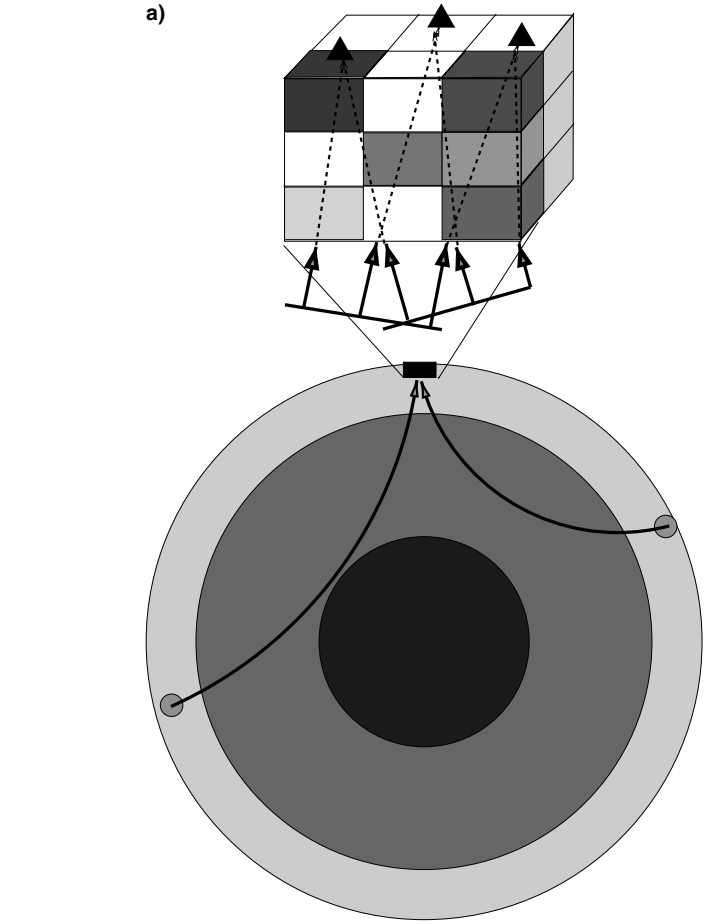
a)

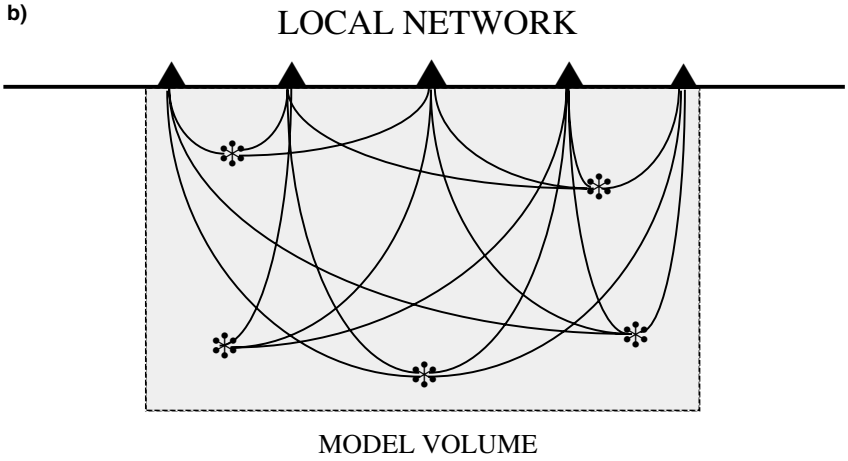
b)
LOCAL NETWORK
MODEL VOLUME

terms, although the equations themselves are more complicated. The equations relating residuals to model parameters can be written directly as

$$t_{ij}^{\text{obs}} - t_{ij}^{\text{cal}} = \sum_k T_{ij}^{(k)} \frac{\Delta u_k}{u_k} + \Delta T_j^o + \frac{\partial T_{ij}}{\partial x_j} \Delta x_j + \frac{\partial T_{ij}}{\partial y_j} \Delta y_j + \frac{\partial T_{ij}}{\partial z_j} \Delta z_j \tag{4}$$

where the dependence of arrival time on source origin time and position is now an explicit part of the system to be solved, entering in the form of the perturbation to origin time (ΔT_j^o) and the partial derivatives of travel time with respect to source coordinates (e.g., $\partial T_{ij}/\partial x_j$) times the corresponding coordinate perturbations (e.g., Δx_j). For a starting model that is a homogeneous and isotropic medium, as assumed in the A&L method, the derivatives are proportional to the corresponding direction cosines of the vector connecting the source to the receiver. For the general case, the derivatives are proportional to the direction cosines of the ray direction at the source (THURBER, 1986).

The original ACH teleseismic and the A&L local earthquake methods both involved single-step linearized inversions for the model parameters. This approach allowed the use of linear inverse theory techniques for model estimation and model resolution and uncertainty analysis. AKI *et al.* (1977) compared models obtained using both a generalized inverse and a stochastic inverse. For the teleseismic case, the system of equations is always linearly dependent due to the trade off between average layer velocity and event origin times, consequently a simple least-squares solution was impossible. The generalized inverse approach uses the non-zero singular values of the $\mathbf{G}^*$ matrix (equation (3)) to compute a least-squares solution, while the stochastic inverse approach computes a damped least-squares solution using a damping value equal to the ratio of the data variance to the solution variance (AKI *et al.*, 1977). AKI and LEE (1976) used just the stochastic inverse approach, because their matrix was nonsingular but contained very small eigenvalues that would amplify the effect of data errors on the model.

Advances in Seismic Tomography

There are a number of important aspects in which the methods and applications of body-wave seismic tomography have been improved over the last 25 years. Some of the advances I will discuss are improvements in the data, development of 3-D ray-tracing techniques, the use of iterative (nonlinear) inversion, the extension to active-

◀

Figure 1

(a) Geometry of the teleseismic tomography method. It is assumed that the *P* waves from teleseisms are incident on the base of the model approximately as plane waves and are recorded on the surface by a dense network. (b) Geometry of the local earthquake tomography method. The model volume contains both the earthquakes and the stations.

source applications, and multiple-method integration. Other improvements include the incorporation of interfaces (e.g., ZHAO *et al.*, 1992) and the use of anisotropic velocity models (e.g., HIRAHARA and ISHIKAWA, 1984).

Better data for tomography have arguably been the most important improvement, because without better data the other advances would have been of relatively limited use. Improvements in data have come in the form of additional instruments, the use of 3-component sensors, and more accurate arrival time picks. These factors allow for improved spatial resolution of structure, the ability to use S waves with reliability, and a sharpening of imaged structure with reduced uncertainty, respectively.

The development of the IRIS PASSCAL program in the U.S. and similar instrument pool developments in other countries has had a tremendously positive impact on the seismic tomography community. In the past, tomography studies were restricted to regions with existing seismic networks (with data access often limited to just those institutions operating the networks) or to a small number of institutions fortunate to have field instruments. Now, any U.S. scientist has the opportunity to propose and, if funded, carry out a seismic field project anywhere in the world involving the collection of seismic data using PASSCAL instruments.

One of the key features of the PASSCAL and other modern instrument pools is that 3-component instruments are the standard. As a result, S waves can be put to use to image structure with nearly the same capability as P waves, the main drawbacks being the presence of the P-coda noise interfering with precise S-wave arrival time picks and the possibility of shear wave splitting adding uncertainties to the data. The main value of S waves is the improved constraint on earthquake locations provided by the addition of S arrivals (GOMBERG *et al.*, 1990), which in turn improves the imaging of structure, and the increased constraints on model interpretation when 3-D models of both V_p and V_s (or V_p/V_s, equivalently Poisson's ratio) are available (EBERHART-PHILLIPS, 1990).

A study by ELLSWORTH (1977) demonstrated that a single-step inversion is adequate for teleseismic tomography when the size of velocity perturbations is relatively modest (less than 10%). The same is generally not true for local earthquake tomography. Beginning with THURBER (1981) and ROECKER (1982), a number of studies using synthetic models and data have shown that an iterative solution incorporating 3-D ray tracing is required for local earthquake tomography. The same is true for cross-borehole travel-time tomography, in which accounting for ray bending is widely recognized as being important. In the local earthquake case, it is even more important due to the coupling between structure and hypocenter locations (KISSLING, 1988; THURBER, 1992).

In the early stages of development, limited computer power made the use of exact ray-tracing techniques impractical. As a result, a variety of approximate ray-tracing techniques were developed (THURBER and ELLSWORTH, 1980; UM and THURBER, 1987; PROTHERO *et al.*, 1988). These methods achieved accuracies approaching that

of reading error (a few tenths of a second or less) for moderate path lengths (up to 60 km), so they remain widely used even today. Over time, efficient exact ray-tracing (or more generally, travel time calculation) methods were developed. Examples include 3-D finite difference (VIDALE, 1988, 1990; PODVIN and LECOMTE, 1991), graph theory (MOSER, 1991), and perturbation methods (VIRIEUX *et al.*, 1988; SNIEDER and SAMBRIDGE, 1992). See THURBER and KISSLING (2000) for a review.

It is important to recognize that even the "exact" methods have limited accuracy. HASLINGER and KISSLING (2001) and KISSLING *et al.* (2001) carried out extensive tests of both exact and approximate ray-tracing techniques, involving reciprocity tests on each method and comparing calculated travel times among methods. The basic conclusion of their analyses is that all methods have comparable accuracy variability for modest path lengths (~60 km), but the "exact" methods are superior for longer path lengths. They also noted that particular care must be taken regarding differences in the way the velocity model is parameterized in order to be able to make accurate comparisons among methods.

Seismic tomography was adapted to controlled-source problems in the 1980s. Non-linear solutions are generally required, as in the local earthquake case. Applications of controlled-source tomography include refraction, cross-borehole, and vertical seismic profiling (VSP). A review of these methods and their applications is beyond the scope of this paper.

Standard seismic tomography using first-arriving waves by itself provides only limited insight into the nature of the subsurface. By its nature, it provides a smoothed image of velocity structure, due to imperfect resolution, wavefront healing, etc. The use of information from secondary arrivals (reflections, conversions) provides one seismic approach for obtaining information about impedance structure, that is, identifying discontinuities. One example will be presented in the following section. Greater insight into the earth's structure can also be gained via multidisciplinary investigations. Two examples of methods that have proven useful in combination with seismic tomography are magnetotellurics (MT) and laboratory and down-hole measurements of seismic properties. EBERHART-PHILLIPS *et al.* (1990) compared velocity and MT models for a 2-D section crossing the San Andreas fault through the 1989 Loma Prieta main shock region (Fig. 2). High-V_p rocks between the San Andreas and Sargent faults were interpreted as mafic rocks due to their high resistivity. Low- V_p rocks in a wedge southwest of the San Andreas were interpreted as over-pressured marine sedimentary rocks due to their very high conductivity. LUTTER *et al.* (1999) compared a refraction-tomography image from the Los Angeles Region Seismic Experiment (LARSE) to well logs (from BROCHER *et al.*, 1998) and laboratory measurements of seismic velocities of representative lithologies (from MCCAFFREE PELLERIN and CHRISTENSEN, 1998) (Fig. 3). The availability of well logs and laboratory data for representative lithologies permitted a detailed interpretation of the tomography image.

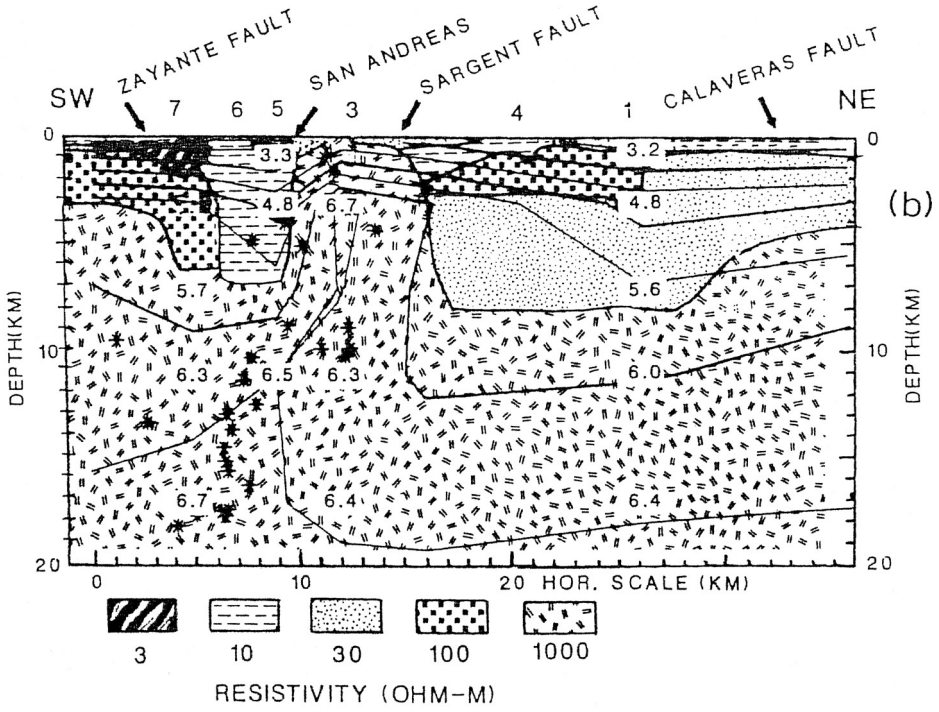

Figure 2
Comparison of a 2-D magnetotelluric model with the corresponding slice through the *P*-wave velocity tomography model contours for the Loma Prieta area (modified from EBERHART-PHILLIPS *et al.*, 1990). Note the excellent correspondence between the low-velocity basin and the low-resistivity units just SW of the San Andreas fault (SAF) and the high-velocity "tongue" and the high resistivity unit between the SAF and Sargent fault.

Applications of Seismic Tomography to Valles Caldera

Volcanic systems have been one of the key targets for seismic tomography studies due to the desire to image the magma chambers at depth in the crust (IYER and DAWSON, 1993). Aki's student Peter Roberts carried out a field project in Valles Caldera in collaboration with Mike Fehler of LANL (also an Aki student). They used six instruments staged in two deployments along a linear profile across the caldera (ROBERTS *et al.*, 1991). Due to their limited teleseismic dataset, they used a forward modeling approach, including *a priori* information on the shallow caldera structure. Their final 2-D P-wave velocity model (Fig. 4) has a lens-shaped crustal low-velocity zone (LVZ) with about a 35% velocity reduction compared to the surrounding rock. The LVZ was interpreted to be the remnants of a cooling magma chamber. The maximum width and minimum thickness of the LVZ are 17 km and 8 km, respectively.

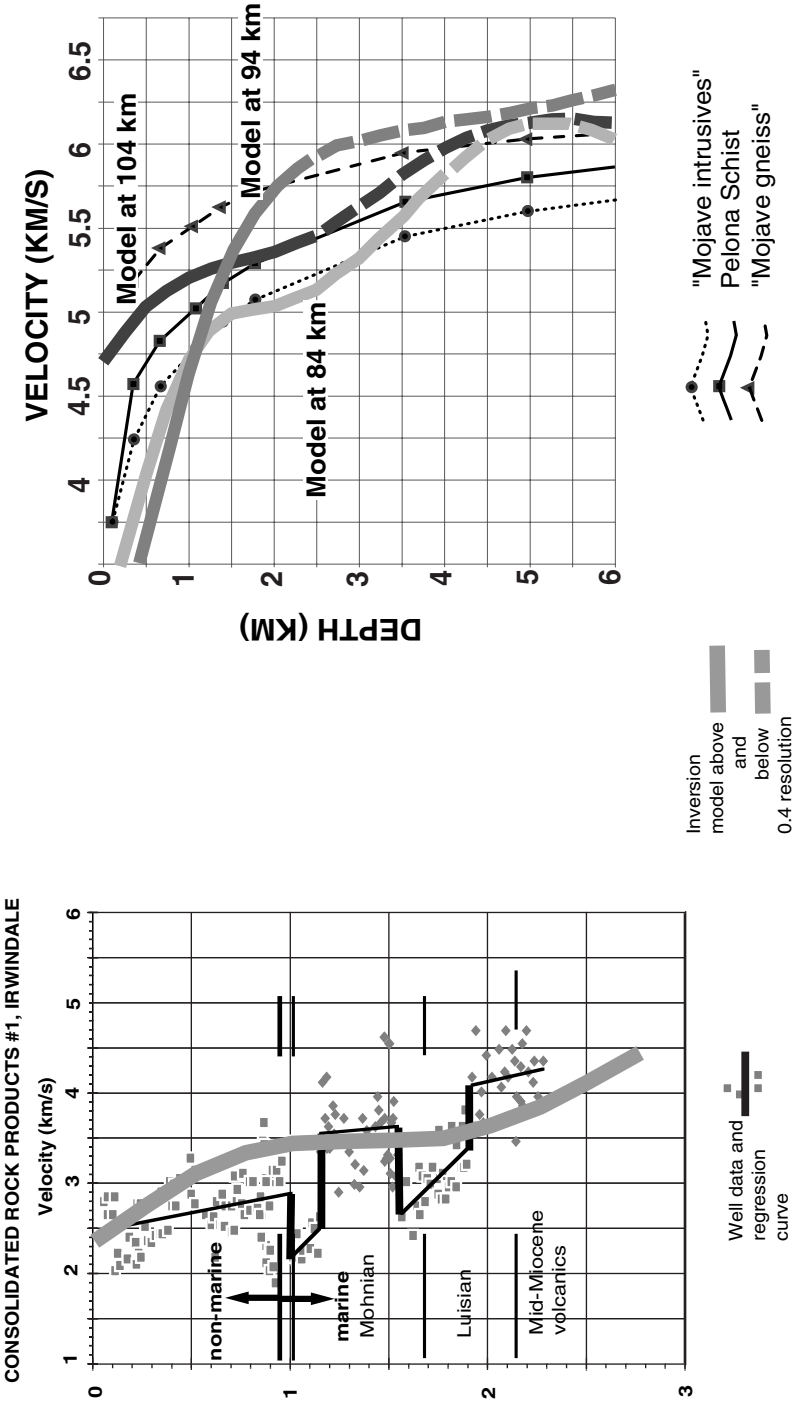

Figure 3
Comparison of velocity profiles through the 2-D LARSE Line 1 *P*-wave velocity model from refraction tomographic and the corresponding well log (left) and laboratory measurements (right) (from LUTTER *et al.*, 1999).

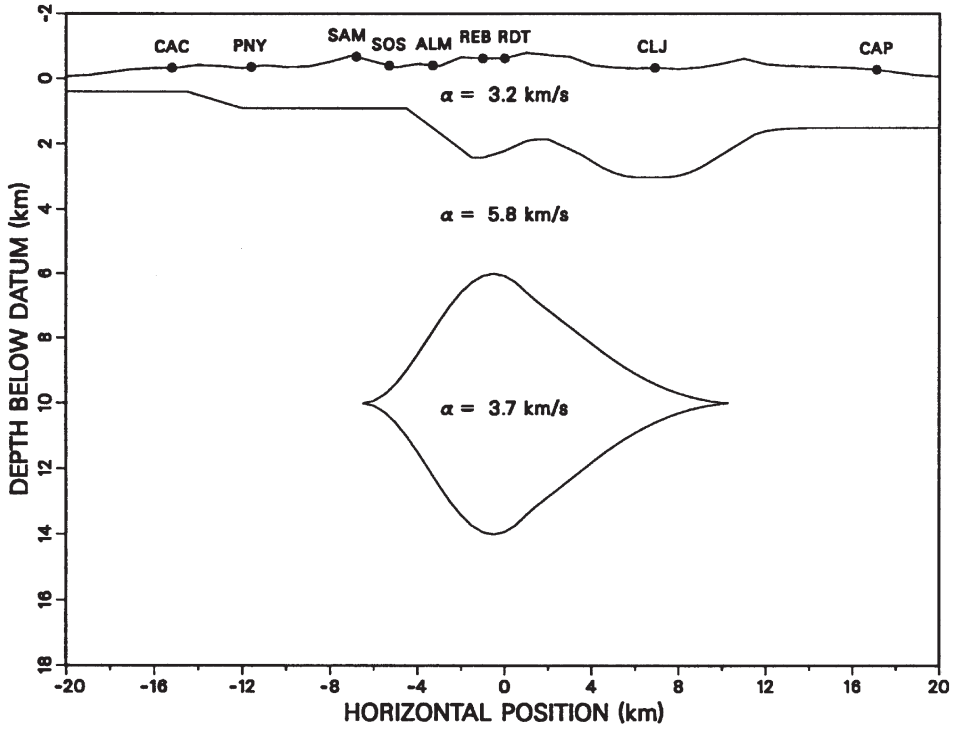

Figure 4
2-D P-wave velocity model for the structure beneath Valles caldera (from ROBERTS *et al.*, 1991). Note the lens-shaped low-velocity zone in the mid-crust (Vp = 3.7 km/s) and the low-velocity caldera fill (Vp = 3.2 km/s).

The results of ROBERTS *et al.* (1991) helped lead to a much larger PASSCAL teleseismic imaging project known as JTEX in the summers of 1993 and 1994. This project involved Peter Roberts, Mike Fehler, and several coworkers an LANL, as well as the author and his research group at UW. The 1993 JTEX pilot experiment, with 22 stations on 2 crossing profiles (LUTTER *et al.*, 1995), provided general confirmation of the location, depth, size, and velocity contrast of the LVZ reported by ROBERTS *et al.* (1991), using the ACH method to derive the velocity model.

With the complete JTEX teleseismic dataset, combining the 1993 and 1994 data (Fig. 5a), STECK *et al.* (1998) modeled the 3-D structure of the caldera using a nonlinear teleseismic tomography method. The principal features in the 3-D model are a mid-crustal low velocity body, roughly $(10\ \text{km})^3$ in size with a –35% velocity contract, consistent with the 2-D results, and a second low velocity body near the Moho (Fig. 5b). The authors combined the tomography model with geochemical information to conclude that Valles Caldera recently received a new pulse of magma from the upper mantle. Neither the 3-D geometry of the Valles magma chamber nor

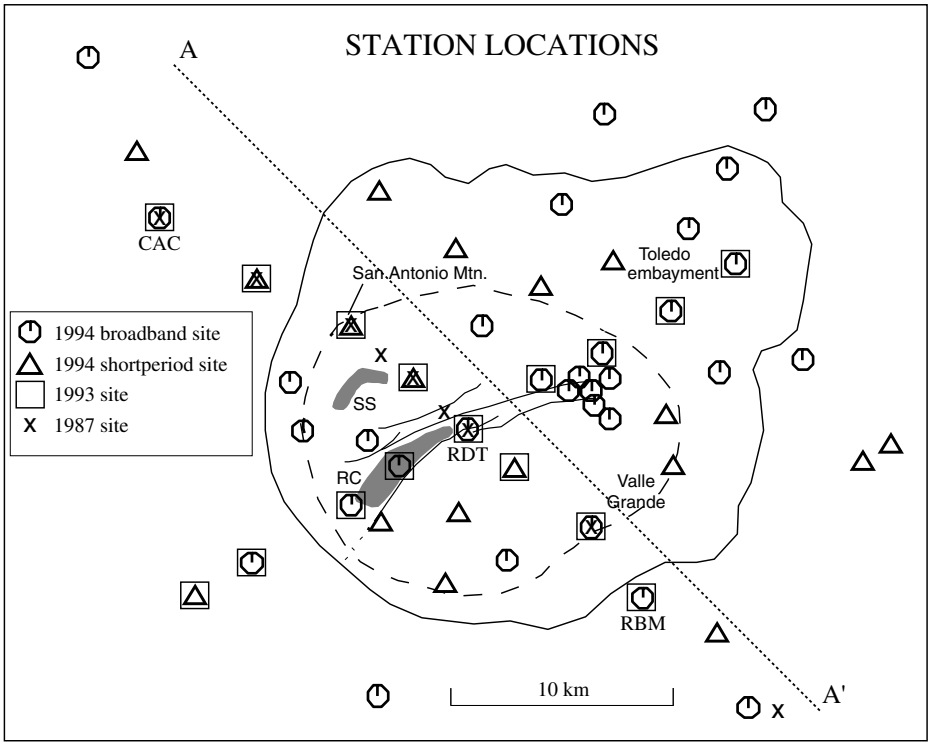

Figure 5a
Layout of the JTEX seismic arrays deployed in 1993 and 1994 (modified from STECK *et al.*, 1998). The solid line indicates the approximate rim of Valles caldera, the dashed line indicates its ring fracture system, and the gray areas indicate the two principle geothermal regions. Section line A-A' is shown in Figures 5b and c.

the presence of the second low velocity body near the Moho could have been resolved without a dense 2-D array of instruments.

Teleseismic first-arrival times are not useful for identifying structural discontinuities in the subsurface, so additional information from the seismograms is required to identify, for example, tops or bottoms of zones of magma. Possible approaches include the use of converted or scattered waves. APREA *et al.* (2002) employed a Kirchhoff migration approach to model the *P*-wave coda of teleseismic waveforms from the JTEX array. Their imaging approach used the surface reflection of the incident *P* wave that subsequently scattered off subsurface structures. This use of the surface-reflected phase for imaging allowed a separation of the target energy from scattered energy from the direct *P* coda. The imaging results (Fig. 5c) show a remarkable correspondence to the main features of the teleseismic tomography image. High amplitudes with opposite polarities are observed from the vicinity of the tops and bottoms of the low-velocity zones imaged by STECK *et al.* (1998).

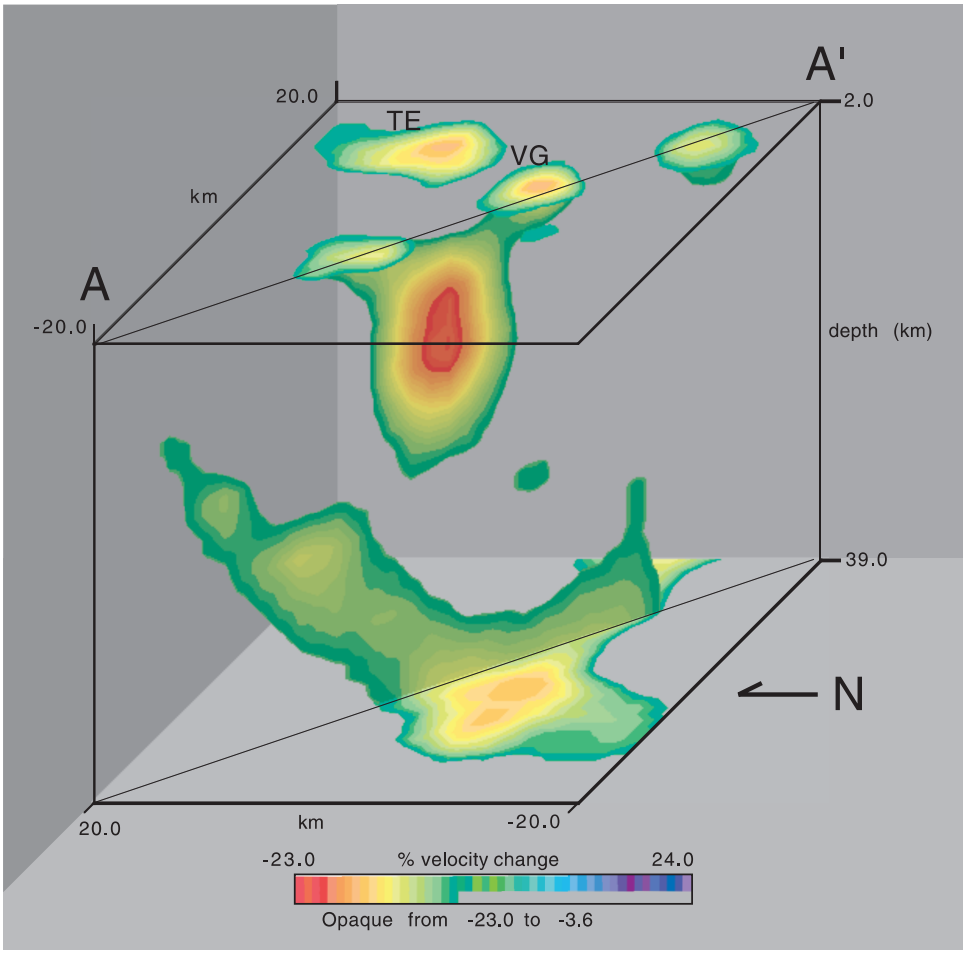

TE = Toledo Embayment, VG = Valle Grande

Figure 5b
Cut-away view of the 3-D model for Valles caldera, showing two low-velocity zones, one in the upper crust and another near the Moho (from STECK *et al.*, 1998).

Applications of Seismic Tomography to the San Andreas Fault

Fault zone studies are another important example for which improved data is vital to improving our understanding. One of the first 3-D local earthquake tomography studies was done by AKI and LEE (1976) along the Bear Valley segment of the San Andreas fault (SAF) in central California, part of the creeping section of the SAF. The data were from the USGS regional network plus a very short-term deployment of portable instruments (long enough to capture 32 local earthquakes),

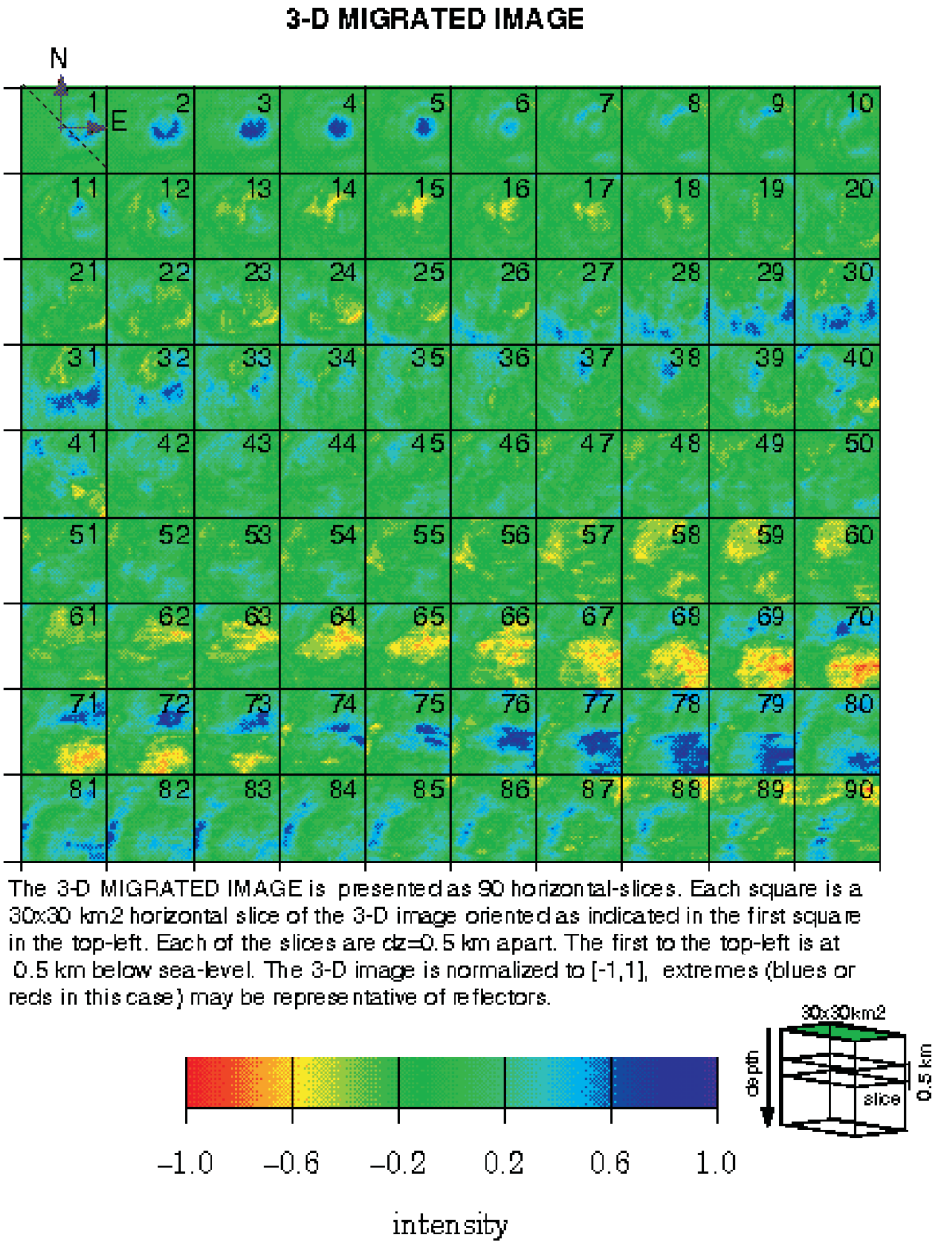

Figure 5c

Horizontal slices through the migrated image from the JTEX waveforms; blues and reds indicate opposite polarity (modified from Aprea *et al.*, 2001). There are anomalies at depths roughly corresponding to the tops and bottoms of the low-velocity zones shown in Figure 5b. Section line A-A' is indicated with a dashed line in the upper left panel (although it extends about 7 km beyond each corner of the panel).

all of which were single-component instruments. The *P*-wave model that could be obtained was very coarse, with block size $3 \times 4 \times 5$ km. The authors were only able to resolve the top layer adequately, nonetheless they were able to image a zone of low velocity paralleling the SAF, with higher velocities on either side (Fig. 6a).

The most puzzling finding of the AKI and LEE (1976) study concerned the earthquake locations. Conventional wisdom held that the SAF is a simple, vertical strike-slip fault in this area, therefore the epicenters should lie along the fault trace. However, whether AKI and LEE (1976) started their inversion with hypocenters aligned on the fault or located several km southwest of the fault, the inversion result had the earthquakes several km southwest of the fault trace (Fig. 6b). Thus either the inversion method is flawed or the SAF is unexpectedly complex in Bear Valley. One possibility is that first-arriving fault zone head waves (BEN-ZION and MALIN, 1991) may be being modeled as direct waves, resulting in location bias. BEN-ZION *et al.* (1992) demonstrate how to use fault zone head waves in an inversion for laterally heterogeneous fault zone structure.

A recent study of a nearby segment of the SAF (also in the central creeping section) indicates how much more information can be obtained with a longer-term

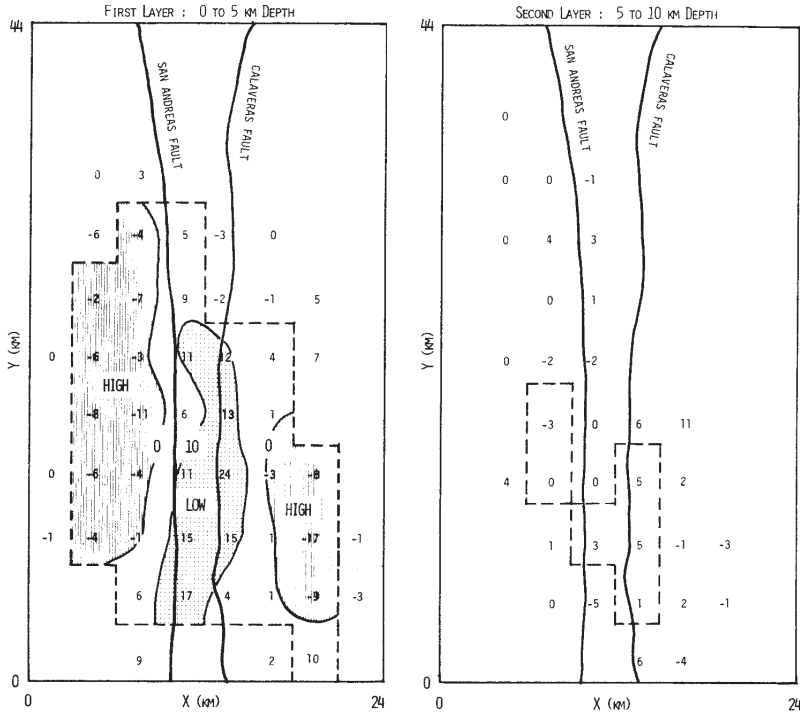

Figure 6a
3-D crustal model for the Bear Valley region of central California, showing a low-velocity fault zone sandwiched between faster basement on either side (modified from AKI and LEE 1976).

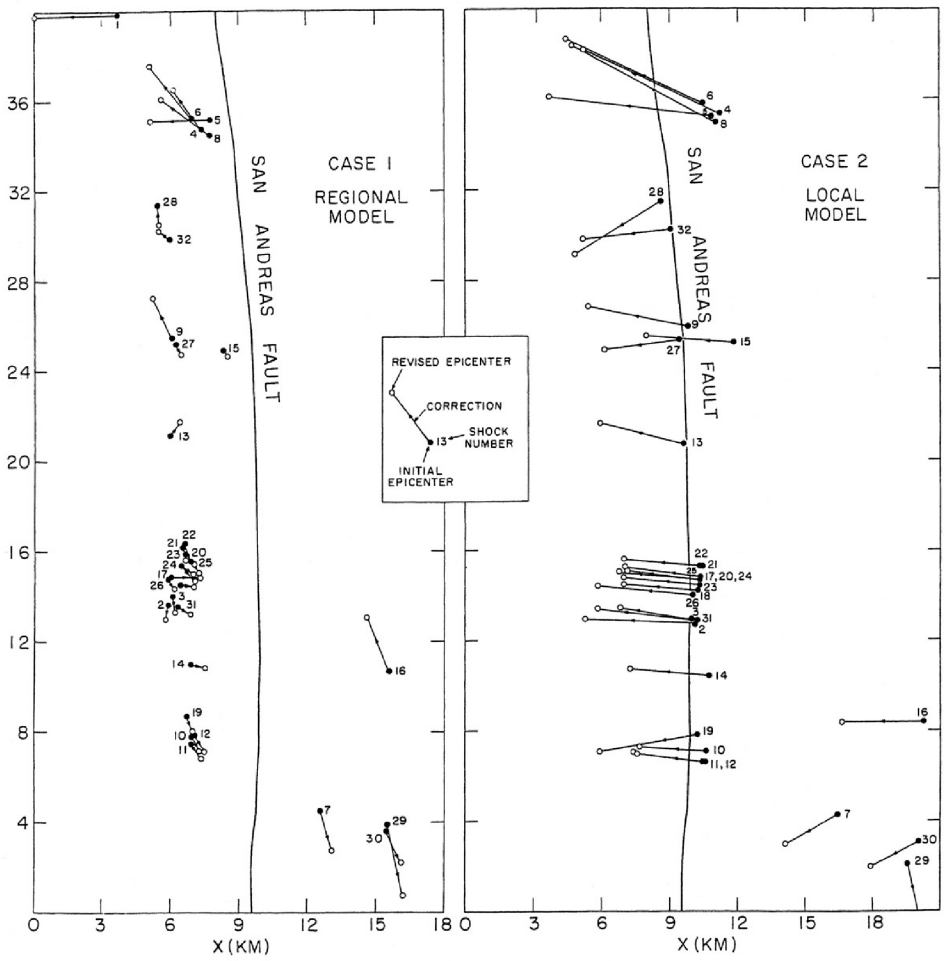

Figure 6b
Earthquake relocation results starting from the "regional" (left) and "local" (right) locations (modified from AKI and LEE 1976). Starting and ending locations are the solid and open circles, respectively. Note the general agreement in the ending locations for the two different sets of starting locations.

deployment of three-component instruments combined with a small active-source experiment (Fig. 7a). The author's research group at UW along with Steve Roecker's group at RPI and Bill Ellsworth (another Aki student) and co-workers at the USGS-Menlo Park deployed 50 PASSCAL instruments for 7 months in a 20×15 km area near Hollister, California, recording hundreds of local earthquakes (THURBER *et al.*, 1997). Their best resolution was along a 2-D section normal to the fault, using a grid size as fine as 1 km. Figure 7b shows their models for V_p and V_p / V_s structure, with seismicity superimposed. They were able to resolve a deep low V_p and high V_p / V_s anomaly in the fault zone,

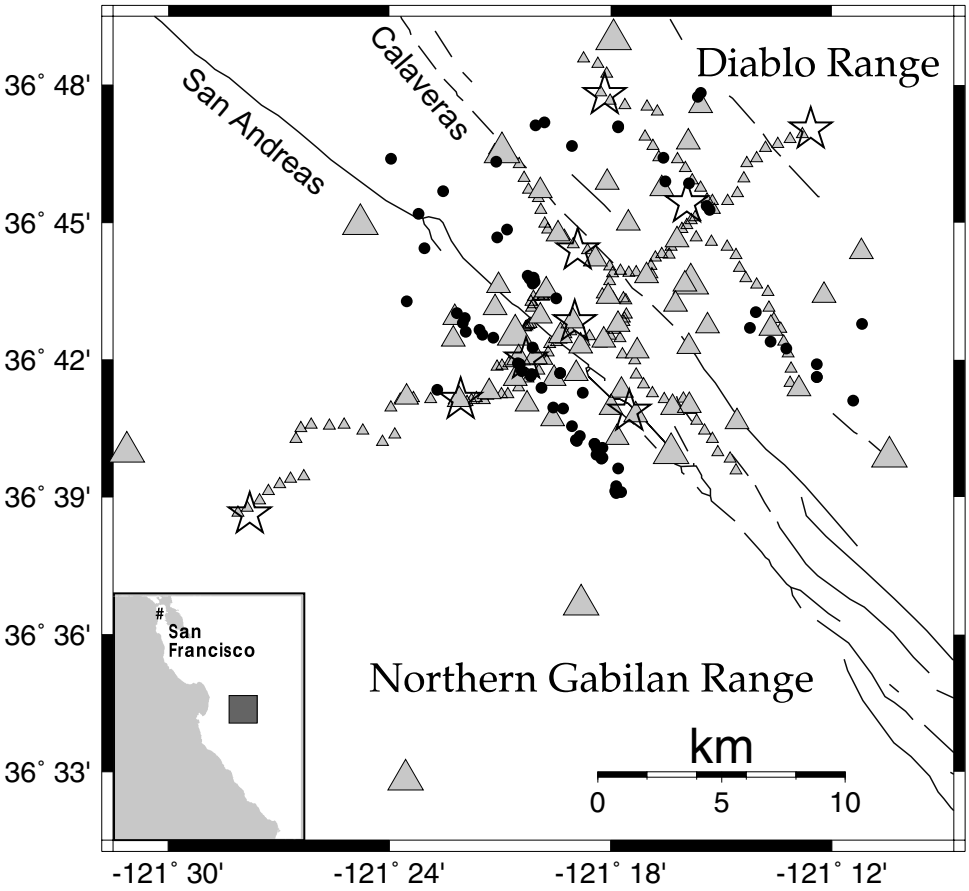

Figure 7a
Layout of the seismic array deployed along the San Andreas fault near Hollister in 1994–1995 (modified from THURBER *et al.*, 1997).

indicative of a highly fractured and probably fluid-rich region. Interestingly, the *P*-wave velocity contrasts across the fault are similar between this study and the original AKI and LEE (1976) study, although they were done along different sections of the SAF. Note how the seismicity is concentrated on the boundary between the high and low V_p regions in Fig. 7a, and how regions of high V_p / V_s are virtually aseismic in Fig. 7b. For this section of the SAF, it appears that the fault dips to the southwest at about 70°.

Other Applications

Although a thorough review of the applications of body-wave seismic tomography would require a book (for example, IYER and HIRAHARA (1993)), it is of value

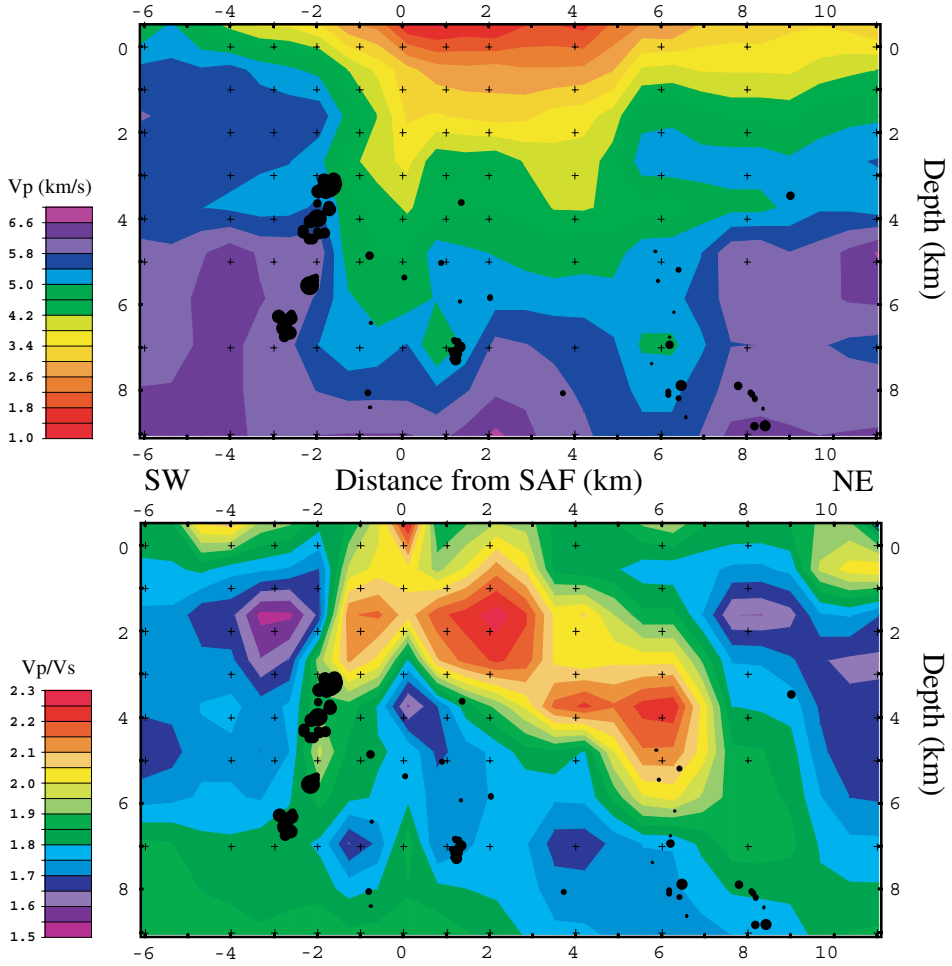

Figure 7b
2-D models of *Vp* (top) and *Vp*/*Vs* (bottom) for the San Andreas fault zone in the Cienega Valley region of central California. The approximate surface trace of the Calaveras fault is about 4 km NE of the SAF. Note the dipping low-velocity/high-*Vp*/*Vs* fault zone, and the concentrations of seismicity adjacent to high-*Vp* zones (modified from THURBER *et al.*, 1997).

to mention some of the highlights achieved over recent decades. Foremost among them is probably the successful imaging of the high-velocity anomalies of downgoing (subducted) slabs, for example by HIRAHARA (1981). Substantial improvement in slab imaging has been obtained by the use of ocean-bottom seismometers (OBS) to augment arrays on land (e.g., HUSEN *et al.*, 2000). OBS controlled-source and local earthquake data has been used to provide remarkable images of mid-ocean ridge structure (e.g., TOOMEY *et al.*, 1990), helping to refine our concept of mid-ocean ridge magma chamber structure and magma propagation. Seismic tomography has also

provided a view of the mantle plume beneath Iceland (WOLFE *et al.*, 1997; ALLEN, 2001). On a global scale, seismic tomography has imaged apparent fossil slabs and other deep-seated anomalies that likely play a fundamental role in global geodynamics (VAN DER HILST *et al.*, 1997). Seismic tomography has also been adapted successfully to surface waves (on local, regional, and global scales), free oscillations, and attenuation (for body and surface waves). Seismic tomography has been one of the most widely and successfully used geophysical tools of the past decade.

Future of Tomography

As we begin the new millennium, there are exciting opportunities for the application and improvement of seismic tomography. If the proposed Earthscope program is initiated (HENYEY *et al.*, 2000), seismic tomography will play important roles in both the USArray and SAFOD components of the program. The plan for the USArray (LEVANDER *et al.*, 1999; MELTZER *et al.*, 1999) is to deploy 400 broadband instruments at about 60–70 km spacing, initially in the southwestern United States. This array would cover about 1/8 of the area of the continental United States at a time. About a year after the array is fully deployed, it will begin to "roll" around the continental United States, eventually providing complete, spatially uniform coverage. The dataset resulting from this effort will provide an exciting opportunity for the application of tomography and other imaging and analysis techniques, providing an unprecedented view of the architecture of the lithosphere beneath the United States. The plan for SAFOD is to drill a deviated borehole to about 3.5 km depth, intersecting the SAF in the immediate vicinity of the rupture patches of small earthquakes. The combination of surface and downhole seismic observations from SAFOD will permit superb tomographic resolution of the fine structure of an active fault zone. The author and Steve Roecker deployed a 15-station PASSCAL array in July 2000, around the proposed drill site for improving earthquake locations, to start the preparations for drilling at Parkfield.

Acknowledgements

The author is grateful to a number of people and government agencies for advice and support, respectively, over the last nearly 25 years of my work on seismic tomography. The list of people starts with Kei Aki, and includes Bill Ellsworth, Steve Roecker, Donna Eberhart-Phillips, Edi Kissling, Gary Pavlis, Steve Taylor, Bob Nowack, Bill Prothero, John Evans, Rob Comer, George Zandt, Wim Spakman, Florian Haslinger, and Stefan Husen. I also thank Florian Haslinger for creating Figure 1a and for a careful reading of the manuscript. I appreciate the constructive

reviews of Tom Parsons, Donna Eberhart-Phillips, and Associate Editor Yehuda Ben-Zion. The list of government agencies supporting my tomography research includes: the National Science Foundation (currently via awards EAR-9814192 and EAR-9814359), with special thanks to Leonard Johnson; the U.S. Geological Survey (currently via award 00HQGR0053); and the Defense Threat Reduction Agency (currently via contract DTRA01-01-C-0085 the content does not necessarily reflect the position or the policy of the U.S. Government, and no official endorsement should be inferred). Finally, I thank Jim Fowler and the staff of the IRIS PASSCAL instrument centers for their dedicated efforts in support of my PASSCAL field projects over the past decade. The facilities of the IRIS Consortium are supported by the National Science Foundation under Cooperative Agreement EAR-0004370.

References

Aki, K. (1982), *Three dimensional Inhomogeneities in the Lithosphere and Asthenosphere: Evidence for Decoupling in the Lithosphere and Flow in the Asthenosphere*, Rev. Geophys. Space Phys. *20*, 161–170.

Aki, K., Christoffersson, A., and Husebye, E.S. (1976), *Three-dimensional Seismic Structure of the Lithosphere under Montana LASA*, Bull. Seism. Soc. Am. *66*, 501–524.

Aki, K., Christoffersson, A., and Husebye, E.S. (1977), *Determination of the 3-dimensional Seismic Structure of the Lithosphere*, J. Geophys. Res. *82*, 277–296.

Aki, K., and Lee, W.H.K. (1976), *Determination of Three-dimensional Anomalies under a Seismic Array Using First P Arrival Times from Local Earthquakes, 1. A Homogeneous Initial Model*, J. Geophys. Res. *81*, 4381–4399.

Allen, R.M. (2001), *The Mantle Plume beneath Iceland and its Interaction with the North-Atlantic Ridge: A Seismological Investigation*, Ph.D. thesis, Princeton University, 184 pp.

Aprea, C.M., Hildebrand, S., Fehler, M., Steck, L. Baldridge, W.S., Roberts, P., Thurber, C.H., and Lutter, W.J. (2002), *3-D Kirchhoff Migration: Imaging of the Jemez Volcanic Field Using Teleseismic Data*, J. Geophys. Res., in press.

Ben-Zion, Y., Katz, S., and Leary, P. (1992), *Joint Inversion of Fault Zone Head Waves and Direct P Arrivals for Crustal Structure near Major Faults*, J. Geophys. Res. *97*, 1943–1951.

Ben-Zion, Y., and Malin, P. (1991), *San Andreas Fault Zone Head Waves near Parkfield, California*, Science *251*, 1592–1594.

Bijwaard, H., Spakman, W., and Engdahl, E.R. (1998), Closing the gap between regional and global travel time tomography, J. Geophys. Res. 103, 30,055–30,078.

Brocher, T.M., Rubel, A.L., Wright, T.L., and Okaya, D.A. (1998), *Compilation of 20 Sonic and Density Logs from 12 Oil Test Wells along LARSE Lines 1 and 2 in the Los Angeles Basin, California*, U.S. Geol. Surv. Open File Rep. *98-366*, 53 pp.

Eberhart-Phillips, D. (1990), *Three-dimensional P and S Velocity Structure in the Coalinga Region, California*, J. Geophys. Res. *95*, 15,343–15,363.

Eberhart-Phillips, D., Labson, V.F., Stanley, W.D., Michael, A.J., and Rodriguez, B.D. (1990), *Preliminary Velocity and Resistivity Models of the Loma Prieta Earthquake Region*, Geophys. Res. Lett. *17*, 1235–1238.

Ellsworth, W.L. (1977), *Three-dimensional Structure of the Crust and Mantle beneath the Island of Hawaii*, Ph.D. Thesis, M.I.T. 327 pp.

Engdahl, E.R. and Lee, W.H.K. (1976), *Relocation of Local Earthquakes by Seismic Ray Tracing*, J. Geophys. Res. *81*, 4400–4406.

Evans, J.R. and Achauer, U. (1993), *Teleseismic velocity tomography using the ACH method: theory and application to continental–scale studies*. In Seismic Tomography (Iyer, H.M., and Hirahara, K., eds.) (Chapman and Hall, London, 1993), pp. 319–360.

FOWLER, J. and PAVLIS, G. (1994), *PASSCAL; A Facility for Portable Seismological Instrumentation*, EOS, Trans. Am. Geophys. Un. Suppl. *75*, 66.

GOMBERG, J.S., SHEDLOCK, K.M., and ROECKER, S.W. (1990), *The Effect of S-wave Arrival Times on the Accuracy of Hypocenter Estimation*, Bull. Seismol. Soc. Am. *80*, 1605–1628.

HASLINGER, F. and KISSLING, E. (2001), *Investigating Effects of 3-D Ray-tracing Methods in Local Earthquake Tomography*, Phys. Earth Plan. Int., in press.

HENYEY, T. and the EARTHSCOPE WORKING GROUP (2000), *Earthscope: A Look into our Continent*, Geotimes *45*, 5 and 40.

HIRAHARA, K. (1981), *Three-dimensional Seismic Structure beneath the Japan Islands and its Tectonic Implications*, J. Phys. Earth *28*, 221–241.

HIRAHARA, K. and ISHIKAWA, Y. (1984), *Travel-time Inversion for Three-dimensional P-wave Velocity Anisotropy*, J. Phys. Earth *32*, 197–218.

HUSEBYE, E.S., CHRISTOFFERSSON, A., AKI K. and POWELL, C. (1976), *Preliminary Results of the 3-dimensional Seismic Structure of the Lithosphere under the USGS Central California Seismic Array*, Geophys. J. Roy. Astron. Soc. *46*, 319–340.

HUSEN, S., KISSLING, E., and FLUEH, E.R. (2000), *Local Earthquake Tomography of Shallow Sudbuction in North Chile: A Combined Onshore and Offshore Study*, J. Geophys. Res. *105*, 28,183–28,198.

IYER, H.M. and DAWSON, P.B. (1993), *Imaging volcanoes using teleseismic tomography*, In *Seismic Tomography*, (Iyer, H.M., and Hirahara, K. eds.), (Chapman and Hall, London, 1993), pp. 466–492.

IYER, H.M. and HIRAHARA, K. (eds.), *Seismic Tomography* (Chapman and Hall, London, 1993), 842 pp.

KISSLING, E. (1988), *Geotomography with Local Earthquake data*, Rev. Geophys. *26*, 659–698.

KISSLING, E., HASLINGER, F., and HUSEN, S. (2001), *Model Parameterization in Seismic Tomography: A Choice of Consequence for the Solution Quality*, Phys. Earth Plan. Int., in press.

LEVANDER, A., HUMPHREYS, E., EKSTRÖM, G., MELTZER, A., and SHEARER, P. (1999), *Proposed Project Would Give Unprecedented Look under North America*, EOS, Trans. Am. Geophys. Un. *80*, 245, 250–251.

LUTTER, W.J., FUIS, G.S., THURBER, C.H., and MURPHY, J.R. (1999), *Tomographic Images of the Upper Crust from the Los Angeles Basin to the Mojave Desert: Results from the Los Angeles Region Seismic Experiment*, J. Geophys. Res. *104*, 25,543–25,565.

LUTTER, W.J., ROBERTS, P.M., THURBER, C.H., STECK, L.K., FEHLER, M.C., STAFFORD, D.G., BALDRIDGE, W.S., and ZEICHERT, T.A. (1995), *Teleseismic P–wave Image of Crust and Upper Mantle Structure beneath the Valles Caldera, New Mexico: Initial Results from the 1993 JTEX Passive Array*, Geophys. Res. Lett. *22*, 505–508.

MASSON, F. and TRAMPERT, J. (1997), *On ACH, or How Reliable is Regional Teleseismic Delay Time Tomography*?, Phys. Earth Planet. Int. *102*, 21–32.

MCCAFFREE, C.L. and CHRISTENSEN, N.I. (1998), *Interpretation of Crustal Seismic Velocities in the San Gabriel-Mojave Region, Southern California*, Tectonophysics *286*, 252–273.

MELTZER, A., RUDNICK, R., ZEITLER, P., LEVANDER, A., HUMPHREYS, G., KARLSTROM, K., EKSTRÖM, G., CARLSON, C., DIXON, T., GURNIS, M., SHEARER, P., and VAN DER HILST, R. (1999), *USArray initiative*, GSA Today *9*, 8–10.

MOSER, T.J. (1991), *Shortest Path Calculation of Seismic Rays*, Geophysics *56*, 59–67.

PAVLIS, G.L. and BOOKER, J.R. (1980), *The Mixed Discrete Continuous Inverse Problem: Application to the Simultaneous Determination of Earthquake Hypocenters and Velocity Structure*, J. Geophys. Res. *85*, 4801–10.

PODVIN, P. and LECOMTE, I. (1991), *Finite Difference Computation of Travel Times in Very Contrasted Velocity Models: A Massively Parallel Approach and its Associated Tools*, Geophys. J. Int. *105*, 271–284.

PROTHERO, W.A., TAYLOR, W.J., and EICKEMEYER, J.A. (1988), *A Fast, Two-point, Three-dimensional Ray-tracing Algorithm Using a Simple Step Search Method*, Bull. Seismol. Soc. Am. *78*, 1190–1198.

ROBERTS, P.M., AKI, K., and FEHLER, M.C. (1991), *A Low-velocity Zone in the Basement Beneath the Valles Caldera, New Mexico*, J. Geophys. Res. *96*, 21,583–21,596.

ROECKER, S.W. (1982), *Velocity Structure of the Pamir–Hindu Kush Region: Possible Evidence of Subducted Crust*, J. Geophys. Res. *87*, 945–959.

SMITH, S.W. (1986), *IRIS: A Program for the Next Decade*, EOS, Trans. Am. Geophys. Un. *67*, 213–219.

SNIEDER, R. and SAMBRIDGE, M. (1992), *Ray Perturbation Theory for Travel Times and Ray Paths in 3-D Heterogeneous Media*, Geophys. J. Int. *109*, 294–322.

SPENCER, C. and GUBBINS, D. (1980), *Travel-time Inversion for Simultaneous Earthquake Location and Velocity Structure Determination in Laterally Varying Media*, Geophys. J. R. Astron. Soc. *63*, 95–116.

STECK, L., THURBER, C., FEHLER, M., LUTTER, W., ROBERTS, P., BALDRIDGE, S., STAFFORD, D., and SESSIONS, R. (1998), *Crust and Upper Mantle P-wave Velocity Structure Beneath the Valles Caldera, New Mexico: Results from the JTEX Teleseismic Experiment*, J. Geophys. Res. *103*, 24,301–24,320.

THURBER, C.H. (1981), *Earth Structure and Earthquake Locations in the Coyote Lake Area, Central California*, Ph.D. Thesis, M.I.T. 331 pp.

THURBER, C.H. (1986), *Analysis Methods for Kinematic Data from Local Earthquakes*, Rev. Geophys. *24*, 793–805.

THURBER, C.H. (1992), *Hypocenter-velocity Structure Coupling in Local Earthquake Tomography*, Phys. Earth Planet. Int. *75*, 55–62.

THURBER, C.H. and ELLSWORTH, W.L. (1980), *Rapid Solution of Ray-tracing Problems in Heterogeneous Media*, Bull. Seismol. Soc. Am. *70*, 1137–48.

THURBER, C.H. and KISSLING, E., *Advances in travel-time calculations for three-dimensional structures*. In *Advances in Seismic Event Location*, (Thurber, C., and Rabinowitz, N., eds.), (Kluwer Academic Publishers, Dordrecht, Netherlands 2000) pp. 71–99.

THURBER, C., ROECKER, S., ELLSWORTH, W., CHEN, Y., LUTTER, W., and SESSIONS, R. (1997), *Two-dimensional Seismic Image of the San Andreas Fault in the Northern Gabilan Range, Central California: Evidence for Fluids in the Fault Zone*, Geophys. Res. Lett. *24*, 1591–1594.

TOOMEY, D.R., PURDY, G.M., SOLOMON, S.C., and WILCOCK, W.S.D. (1990), *The Three-dimensional Seismic Velocity Structure of the East Pacific Rise near Latitude 9° 30' N*, Nature *347*, 639–645.

UM, J. and THURBER, C.H. (1987), *A Fast Algorithm for Two-point Seismic Ray Tracing*, Bull. Seismol. Soc. Am. *77*, 972–986.

VAN DER HILST, R.D., WIDIYANTORO, S., and ENGDAHL, E.R. (1997), *Evidence for Deep Mantle Circulation from Global Tomography*, Nature *386*, 578–584.

VIDALE, J.E. (1988), *Finite-difference Travel-Time Calculation*, Bull. Seis. Soc. Am. *78*, 2062–2076.

VIDALE, J.E. (1990), *Finite-difference Calculation of Travel Times in Three Dimensions*, Geophysics *55*, 521–526.

VIRIEUX, J., FARRA, V., and MADARIAGA, R. (1988), *Ray Tracing for Earthquake Location in Laterally Heterogeneous Media*, J. Geophys. Res. *93*, 6585–6599.

WIDIYANTORO, S., and VAN DER HILST, R. (1997), *Mantle Structure beneath Indonesia Inferred from High-resolution Tomographic Imaging*, Geophys. J. Int. *130*, 167–182.

WOLFE, C.J., BJARNASON, I.T., VAN DECAR, J.C., and SOLOMON, S.C. (1997), *Seismic Structure of the Iceland Mantle Plume*, Nature, *385*, 245–247.

ZHAO, D., HASEGAWA, A., and HORIUCHI, S. (1992), *Tomographic Imaging of P- and S- wave Velocity Structure beneath Northeastern Japan,* J. Geophys. Res. *97*, 19,909–19,928.

(Received July 1, 2000, accepted January 31, 2001)